JOURNAL OF COMPUTATIONAL PHYSICS **127,** 179–195 (1996)
ARTICLE NO. 0167

A Variational Level Set Approach to Multiphase Motion*

HONG-KAI ZHAO, T. CHAN, B. MERRIMAN, AND S. OSHER

Mathematics Department, UCLA, Los Angeles, California 90095-1555

Received July 31, 1995; revised February 22, 1996

A coupled level set method for the motion of multiple junctions (of, e.g., solid, liquid, and grain boundaries), which follows the gradient flow for an energy functional consisting of surface tension (proportional to length) and bulk energies (proportional to area), is developed. The approach combines the level set method of S. Osher and J. A. Sethian with a theoretical variational formulation of the motion by F. Reitich and H. M. Soner. The resulting method uses as many level set functions as there are regions and the energy functional is evaluated entirely in terms of level set functions. The gradient projection method leads to a coupled system of perturbed (by curvature terms) Hamilton–Jacobi equations. The coupling is enforced using a single Lagrange multiplier associated with a constraint which essentially prevents (a) regions from overlapping and (b) the development of a vacuum. The numerical implementation is relatively simple and the results agree with (and go beyond) the theory as given in [12]. Other applications of this methodology, including the decomposition of a domain into subregions with minimal interface length, are discussed. Finally, some new techniques and results in level set methodology are presented.

1. INTRODUCTION

In this article we shall develop an algorithm for the motion of multiple junctions which is associated with an energy functional involving the length of each interface and the area of each subregion. (Three-dimensional analogues are also easy to implement—the word ''area'' replaces ''length'' and ''volume'' replaces ''area'' in the above). Examples of such motion include solid, liquid, grain, or multiphase boundaries. These internal interfaces are generally out of equilibrium and the resulting motion is driven by decreasing energy.

The simplest model involves three curves meeting at a point as shown in Fig. 1. Each interface Γ_{ij} separates regions Ω_i and Ω_j and the normal velocity is a positive multiple of the curvature of the interface plus the difference of the bulk energies.

$$\text{Normal velocity of } \Gamma_{ij} = v_{ij} = f_{ij}\kappa_{ij} + (e_i - e_j). \quad (1.1)$$

* Research supported by ARPA/ONR-N00014-92-J-1890, NSF DMS94-04942, and ARO DAAH04-95-1-0155.

The point at which they meet (the triple junction) has prescribed angles which can be shown [12] to be defined by

$$\frac{\sin\theta_1}{f_{23}} = \frac{\sin\theta_2}{f_{31}} = \frac{\sin\theta_3}{f_{12}}, \quad (1.2)$$

where θ_i is the angle between the two curves Γ_{ij} and $\Gamma_{ij'}$, $j \neq j'$; see Fig. 1.

This problem was defined and analyzed clearly in a paper by Reitich and Soner [12], and we base our approach in part on their theoretical framework. Their method does not lend itself to a direct numerical treatment.

Our objective here is to develop and implement numerical algorithms which ''capture'' rather than ''track'' the interfaces, based on the level set method of Osher and Sethian [9]. The usual advantages of the level set method hold (see, e.g., [2, 8, 9, 16]). In the case of a single interface separating two phases the central idea is to follow the evolution of a function ϕ, whose zero-level set corresponds to the position of the moving interface. The method permits cusps, corners, and topological changes.

Since its inception, the method has been used to compute and analyze an array of mathematical and physical phenomena. See, e.g., [8] and the references theorem.

In earlier work [6], Merriman, Bence, and Osher have extended the level set method to compute the motion of multiple junctions. Also in that paper, and in [5, 7], a simple method based on the diffusion of characteristic functions of each set Ω_i, followed by a certain reassignment step, was shown to be appropriate for the motion of multiple junctions in which the bulk energies are zero (and, hence, the constants $e_i = 0, i = 1, ..., n$) and the f_{ij} are all equal to the same positive constant, i.e., pure mean curvature flow.

More general motion involving somewhat arbitrary functions of curvature, perhaps different for each interface was proposed in [6] as well. This was implemented basically by decoupling the motions and then using a reassignment step. Again each region has its own private level set function. This function moves each level set with a normal velocity depending on the proximity to the nearest interface, thus vacuum and overlapping regions generally de-

0021-9991/96 $18.00

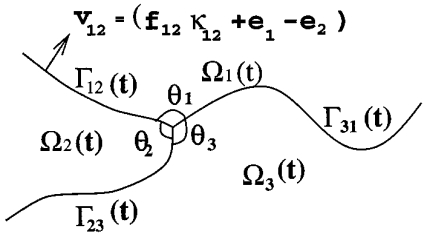

FIG. 1. The interfaces Γ_{ij} with normal velocity $v_{ij} = f_{ij}\kappa_{ij} + e_i - e_j$ and angle θ_i.

velop. Then a simple reassignment step is used, removing all the vacuum and overlap. For details see [6]. In that paper there was no restriction to gradient flows. However, the general method in [6] lacks (so far) a clean theoretical basis to guide the design of numerical algorithms. We rectify this with the present method.

Here we follow Reitich and Soner's variational formulation in [12]. Given a disjoint family Ω_i of regions in R^2 with the common boundary between Ω_i and Ω_j denoted by Γ_{ij}, we associate to this geometry an energy function of the form

$$\begin{aligned} E &= E_1 + E_2 \\ E_1 &= \sum_{1\le i\le j\le n} f_{ij}\,\text{length}\,(\Gamma_{ij}) \\ E_2 &= \sum_{1\le i\le n} e_i\,\text{area}\,(\Omega_i) \end{aligned} \tag{1.3}$$

where E_1 is the energy of the interface (surface tension), E_2 is bulk energy, and n is the number of phases. The gradient flow induces motion such that the normal velocity of each interface is defined in (1.1). At triple points (which can be seen geometrically by the triangle inequality to be the only stable junctions if all the $f_{ij} > 0$), the angles are determined by (1.2) throughout the motion. (It is interesting that our numerical method, defined in the following sections, does this automatically. The speed of propagation of the angle into the equilibrium of this configuration is infinite.) Reitich and Soner make both these statements—we provide the details for (1.1) in the next section, and the derivation of (1.2) is rather straightforward and will not be given here.

To summarize, there are two main points to this paper:

(1) We develop an efficient and versatile computational algorithm for the theoretical variational problem posed by Reitich and Soner in [12].

(2) We provide a theoretical basis, as a descent solution to a variational problem, for the time split level set method proposed by Merriman, Bence, and Osher in [6], which in turn allows us to develop a superior version of that original ad hoc algorithm.

The format of our paper is as follows. In the next section, we give the level set formulation for the dynamics of the motion and discuss other applications such as the optimal decomposition of domains. In Section 3 we give the details of the numerical implementation. In Section 4 we present the numerical results. Finally, in the Appendix we discuss some useful new results and techniques concerning the level set methodology.

2. THE LEVEL SET FORMULATION

For a given open region Ω with smooth boundary we assume the existence of a level set function $\varphi(x, y)$, which is Lipschitz continuous, satisfying

$$\varphi(x, y) > 0 \quad \text{for } (x, y) \in \Omega \tag{2.1a}$$

$$\varphi(x, y) = 0 \quad \text{for } (x, y) \in \partial\Omega \tag{2.1b}$$

$$\varphi(x, y) < 0 \quad \text{for } (x, y) \in \overline{\Omega}^c. \tag{2.1c}$$

Then we have the simple facts,

$$\text{length}\,(\partial\Omega) = \int\int \delta(\varphi(x, y))|\nabla\varphi(x, y)|dx\,dy \tag{2.2a}$$

$$\text{area}\,(\Omega) = \int\int H(\varphi(x, y))\,dx\,dy, \tag{2.2b}$$

$$\begin{aligned} &\text{curvature of any level set of } \phi \text{ at a point } (x, y) \\ &\quad = -\nabla\cdot(\nabla\varphi/|\nabla\varphi|), \end{aligned} \tag{2.2c}$$

where $H(x)$ is the Heaviside function

$$H(x) = \begin{cases} 1, & x \ge 0 \\ 0, & x < 0 \end{cases}$$

and $\delta(x)$ is the Dirac delta function

$$\delta(x) = \frac{d}{dx}H(x) \quad \text{(in the sense of distributions)}.$$

Of course, our numerical simulations involve slightly regularized versions of $\delta(x)$ and $H(x)$—see (3.4) below.

Here, and throughout this paper, we define

$$|\nabla\varphi| = \sqrt{\varphi_x^2 + \varphi_y^2}.$$

The statement in (2.2b) is obvious, while that in (2.2a) was proven in [2], for example.

Given n different regions (phases), which are moving in time, we associate to each regions $\Omega_i(x, y, t)$ a level set function $\varphi_i(x, y, t)$ and define

$$E = E_1 + E_2 \tag{2.3a}$$

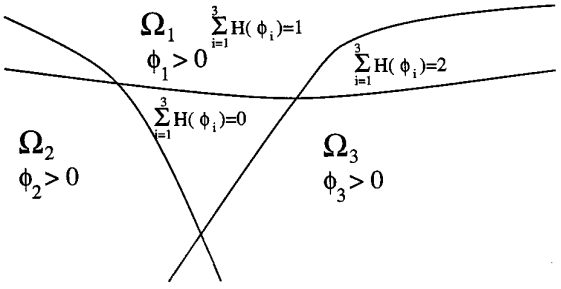

FIG. 2. Regions of vacuum or overlap.

$$E = E_1 + E_2 \tag{2.3b}$$

$$E_1 = \sum_{i=1}^{n} \gamma_i \int\int \delta(\varphi_i(x_i, y, t))|\nabla\varphi_i(x, y, t)|dx\,dy \tag{2.3c}$$

$$E_2 = \sum_{i=1}^{n} e_i \int\int H(\varphi_i(x, y, t))\,dx\,dy,$$

where

$$f_{ij} = \gamma_i + \gamma_j, \quad 1 \le i < j \le n. \tag{2.3d}$$

In the (most interesting) case when $n = 3$ we can solve uniquely for the γ_i. For $n > 3$, (2.3d) restricts our class of admissible surface energies f_{ij}. We shall discuss this relation further below in (2.7) and (2.8) and in the remarks which follow those equations. (We note here that, by allowing the γ_i to depend on all of the φ_j, we can handle the cases $n \ge 4$. This will be discussed in future work.) It is clear from (2.2) that (1.3) and (2.3) are equivalent. Now our problem becomes:

Minimize E subject to the constraint that

$$\sum_{i=1}^{n} H(\varphi_i(x, y)) - 1 \equiv 0. \tag{2.4}$$

This infinite set of constraints prevents the development of overlapping regions and/or vacuum. It requires that the level curves $\{(x, y)|\varphi_i(x, y, t) = 0\}$ match perfectly. See Fig. 2.

The implementation of (2.3) with the infinite set of constraints (2.4) is computationally demanding. Instead we try to replace the constraint (2.4) by a single constraint

$$\int\int \frac{(\sum H(\varphi_i(x, y, t)) - 1)^2}{2}\,dx\,dy = 0. \tag{2.5}$$

We shall show below (and it is intuitively clear) that this is not legitimate—one cannot replace an arbitrary number of constraints by the single constraint obtained by summing their squares. Doing that results in a degenerate constraint, i.e., one which is unsuitable for use with Lagrange multipliers because the gradient of the constraint function vanishes identically on the constraint manifold. See the discussion after Remark 2.6. Instead we shall enforce

$$\int\int \frac{(\sum H(\varphi_i(x, y, t)) - 1)^2}{2}\,dx\,dy = \varepsilon \tag{2.6}$$

for $\varepsilon > 0$, as small as we can manage numerically. (We find that ε corresponds to the area of one grid cell for our computations. Throughout this paper, $\varepsilon > 0$ will denote various small positive numbers).

In the first version of this paper we proposed a reassignment step, similar to that in [6], in which at the end of each calculation we remove the very small vacuum and (perhaps) overlap region. We have since found that this is unnecessary numerically for situations in which all the $\gamma_i > 0$. If some of the $\gamma_i = 0$, we set them to the value $C\,\Delta x$, for C an $O(1)$ constant and Δx = grid size. The numerical evidence is that this regularization with "vanishing viscosity" removes the need for reassignment. We typically have a one point vacuum region, which leads to $\varepsilon = O(\Delta x)^2$ in (2.6). We justify the need for this explicit use of vanishing viscosity in the Appendix. We remark here that this is quite unlike the single level set case developed in [9] and discussed in many succeeding papers, where the inviscid limit comes automatically through the finite difference approximation of the convection term. See the Appendix for a further discussion of this.

Remark 2.1. The formulations (2.3) and (1.3) can be extended to the case where the e_i, γ_i, and f_{ij} are functions of the space variables.

Using the angle relation (1.2) at a triple point, we can set (normalizing $\sin\theta_1/f_{23} = 1$):

$$\gamma_2 + \gamma_3 = \sin\theta_1 \tag{2.7a}$$

$$\gamma_3 + \gamma_1 = \sin\theta_2 \tag{2.7b}$$

$$\gamma_1 + \gamma_2 = \sin\theta_3, \tag{2.7c}$$

leading us to

$$\gamma_1 = \frac{\sin\theta_3 + \sin\theta_2 - \sin\theta_1}{2} = \frac{\sin\theta_3(1 + \cos\theta_2)}{2} + \frac{\sin\theta_2(1 + \cos\theta_3)}{2} \tag{2.8a}$$

$$\gamma_2 = \frac{\sin\theta_1 + \sin\theta_3 - \sin\theta_2}{2} = \frac{\sin\theta_1(1 + \cos\theta_3)}{2} + \frac{\sin\theta_3(1 + \cos\theta_1)}{2} \tag{2.8b}$$

$$\gamma_3 = \frac{\sin\theta_2 + \sin\theta_1 - \sin\theta_3}{2} = \frac{\sin\theta_2(1+\cos\theta_1)}{2} + \frac{\sin\theta_1(1+\cos\theta_1)}{2}. \tag{2.8c}$$

Thus the γ_i are all positive iff all the angles θ_i are between 0° and 180°. The importance of this is seen in the evolution equation (2.12) we shall derive below.

We now state a first-order necessary condition for our minimization problem.

THEOREM 2.1. *The solutions to the minimization problem*:

M: *minimize* $E_1 + E_2$ (*of* 2.3) *in a fixed domain D subject to the integral constraint* (2.6),

satisfy, *for* $i = 1, ..., n$

$$\delta(\varphi_i)\left(\gamma_i\nabla\cdot\left(\frac{\nabla\varphi_i}{|\nabla\varphi_i|}\right) - e_i - \lambda\left(\sum_{i=1}^{n} H(\varphi_i) - 1\right)\right) = 0 \tag{2.9a}$$

with boundary conditions

$$\frac{\delta(\varphi_i)}{|\nabla\varphi_i|}\frac{\partial\varphi_i}{\partial n} = 0 \quad \text{on } \partial D, \tag{2.9b}$$

where λ *is a Lagrange multiplier*.

Proof. Using the Lagrange multiplier, the solution minimizes the functional

$$f(\varphi_1, ..., \varphi_n) = \int\int_D \left[\sum_{i=1}^{n} \gamma_i\delta(\varphi_i(x,y,t))|\nabla\varphi_i(x,y,t)| + \sum_{i=1}^{n} e_i H(\varphi_i(x,y,t)) + \frac{\lambda}{2}\left(\sum_{i=1}^{n} H(\varphi_i(x,y,t)) - 1\right)^2\right] dx\,dy. \tag{2.10}$$

The Frechet derivative of f with respect to ϕ_i in the $\psi(x, y)$ direction is (2.11)

$$\begin{aligned}\left(\frac{\partial f}{\partial\phi_i}, \psi\right) &= \int\int_D \gamma_i\left(\delta'(\phi_i)|\nabla\phi_i|\psi + \delta(\phi_i)\frac{\nabla\phi_i\cdot\nabla\psi}{|\nabla\phi_i|} + e_i\delta(\phi_i)\psi + \lambda\left(\sum_{j=1}^{n} H(\phi_j) - 1\right)\delta(\phi_i)\psi\,dx\,dy\right.\\ &= \int\int_D \left[\gamma_i\left(\delta'(\phi_i)|\nabla\phi_i| - \nabla\cdot\left(\delta(\phi_i)\frac{\nabla\phi_i}{|\nabla\phi_i|}\right)\right) + e_i\delta(\phi_i) + \lambda\left(\sum_{j=1}^{n} H(\phi_j) - 1\right)\delta(\phi_i)\right]\psi\,dx\,dy \\ &\quad + \int_{\partial D}\frac{\delta(\phi_i)}{|\nabla\phi_i|}\frac{\partial\phi_i}{\partial n}\psi\,ds \\ &= -\int\int_D \delta(\phi_i)\left(\gamma_i\nabla\cdot\left(\frac{\nabla\phi_i}{|\nabla\phi_i|}\right) - e_i - \lambda\left(\sum_{i=1}^{n} H(\phi_i) - 1\right)\right)\psi\,dx\,dy \\ &\quad + \int_{\partial D}\frac{\delta(\phi_i)}{|\nabla\phi_i|}\frac{\partial\phi_i}{\partial n}\psi\,dx. \quad \blacksquare\end{aligned} \tag{2.11}$$

This expression must vanish for all $\varphi(x, y)$. Thus we obtain (2.9).

We wish to solve this constrained optimization problem by using the gradient projection method of Rosen [13], where we parametrize the descent direction by time and rescale, replacing the common factor $\delta(\varphi_i)$ by $|\nabla\varphi_i|$. This time rescaling does not affect the steady state solution, but it does remove stiffness near the zero level sets of φ_i. Only the speed of descent, not its direction, is affected. We get the following system of nonlinear evolution equations for the minimization:

$$\frac{\partial\varphi_i}{\partial t} = |\nabla\varphi_i|\left(\gamma_i\nabla\cdot\left(\frac{\nabla\varphi_i}{|\nabla\varphi_i|}\right) - e_i - \lambda\left(\sum_{j=1}^{n} H(\varphi_j) - 1\right)\right) \quad \text{in } D \text{ for } i = 1, 2 ..., n, \tag{2.12a}$$

with the boundary conditions

$$\frac{\partial\varphi_i}{\partial n} = 0 \quad \text{on } \partial D. \tag{2.12b}$$

The Lagrange multiplier λ is updated using Rosen's idea, which essentially requires that the φ_i's, determined by (2.12), satisfy the constaint (2.5):

$$\begin{aligned}\frac{1}{2}\frac{d}{dt}\int\int_D\left(\sum_{i=1}^{n} H(\phi_i(x,y,t)) - 1\right)^2 dx\,dy &= 0 \\ &= \sum_{i=1}^{n}\int\int_D\left(\sum_{j=1}^{n} H(\phi_j) - 1\right)\delta(\phi_i)\frac{\partial\phi_i}{\partial t}\,dx\,dy \\ &= \sum_{i=1}^{n}\int\int_D\left(\sum_{j=1}^{n} H(\phi_j) - 1\right)\delta(\phi_i)|\nabla\phi_i| \\ &\quad \left(\gamma_i\nabla\cdot\left(\frac{\nabla\phi_i}{|\nabla\phi_i|}\right) - e_i - \lambda\left(\sum_{j=1}^{n} H(\phi_j) - 1\right)\right)dx\,dy.\end{aligned} \tag{2.13}$$

So we get

$$\lambda = \frac{\sum_{i=1}^{n} \int\int_D \delta(\phi_i)|\nabla\phi_i| \left(\gamma_i \nabla \cdot \left(\frac{\nabla\phi_i}{|\nabla\phi_i|}\right) - e_i\right) \left(\sum_{j=1}^{n} H(\phi_j) - 1\right) dx\, dy}{\sum_{i=1}^{n} \int\int_D \delta(\phi_i)|\nabla\phi_i| \left(\sum_{j=1}^{n} H(\phi_j) - 1\right)^2 dx\, dy}. \tag{2.14}$$

We need to show that the rescaling works in the following sense.

LEMMA 2.1. *$\partial E/\partial t \le 0$, given* (2.12) *and* (2.14).

Proof. We use the identity

$$\begin{aligned}
\frac{\partial E}{\partial t} &= \int\int_D \left[\sum_{i=1}^{n} \gamma_i \left((\varphi_i)_t \delta'(\varphi_i)|\nabla\varphi_i| + \delta(\varphi_i) \frac{\nabla\varphi_i}{|\nabla\varphi_i|}(\nabla\varphi_i)_t\right) + e_i(\varphi_i)_t \delta(\varphi_i)\right] \\
&= \int\int \left[\sum_{i=1}^{n} (\varphi_i)_t \left[\delta(\varphi_i)\left[e_i - \gamma_i \nabla \cdot \frac{\nabla\varphi_i}{|\nabla\varphi_i|}\right]\right]\right] \qquad (2.15) \\
&= -\int\int \sum_{i=1}^{n} \delta(\varphi_i)|\nabla\varphi_i| \left[\left[\gamma_i \left(\nabla \cdot \left(\frac{\nabla\varphi_i}{|\nabla\varphi_i|}\right)\right) - e_i\right]^2 \right. \\
&\quad \left. - \lambda \left(\sum_{j=1}^{n} H(\varphi_j) - 1\right)\left[\gamma_i \nabla \cdot \left(\frac{\nabla\varphi_i}{|\nabla\varphi_i|}\right) - e_i\right]\right].
\end{aligned}$$

We recognize that every integral above is merely a line integral, along the zero level set of the corresponding φ_i, of the quantity following $|\nabla\varphi_i|$ above. The result follows from (2.14) and Schwarz' inequality—see Remark 2.6 below for a related, more general argument.

Remark 2.2. The geometric interpretation of the induced motion is as follows:

Each level set of each function φ_i moves normal to itself with normal velocity:

$$\begin{aligned}
(v_i)_n = \gamma_i\,&(\text{total curvature of level set}) - e_i - \lambda \\
&(\text{total amount of overlap among all regions} \\
&- \text{amount of vacuum between all regions}).
\end{aligned} \tag{2.16}$$

Of course, we are only interested in the zero level set, which must coincide with all interfaces Γ_{ij}, $j \neq i$, if the method is to work. The only coupling of this curvature regularized system of Hamilton–Jacobi equations comes through the single constraint.

The curvature terms tend to straighten out the curves—this acts like surface tension or tangential diffusion—while the constant terms try to move the curve normal to itself uniformly. The multiple junction interaction comes from the terms which include the Lagrange multiplier.

Remark 2.3. This motion was analyzed (using an abstract variational different formulation in terms of curves and areas, not level sets, and only for the $n = 3$ case) by Reitich and Soner [12]. If each of the $\gamma_i > 0$, there is a unique viscosity solution. Obviously, negative γ_i will give disastrous instabilities. If $\gamma_i \equiv 0$ they demonstrate nonuniqueness of this problem, very much in the spirit of nonuniqueness of solutions to scalar Hamilton–Jacobi equations without the viscosity solution regularization. Also in that spirit, they prove uniqueness of the inviscid ($\gamma_i \equiv 0$) case by letting $\varepsilon\gamma_i$ be the coefficients with $\varepsilon \downarrow 0$. We shall demonstrate numerically that our method also picks out this unique limit solution, unlike what was proposed in [17]. Again this is in the spirit of Sethian's entropy condition [14] as formulated in [9] for the motion of a single front. However, the numerical implementation is different from the single front case. Reitich and Soner's analysis does not easily lend itself to a numerical implementation. See the Appendix for a further discussion of the $\gamma_i \equiv 0$ case.

Remark 2.4. Note that, as expected, the equations of motion are independent of the choice of level set function φ. In particular, if $h(\varphi)$ is an increasing function, with $h(0) = 0$, then the system (2.12), (2.14) is invariant for $\psi = h(\varphi)$. This reflects the fact that only level sets matter, not the point values of the representing function.

Remark 2.5. If we can set $\varphi_i = d_i$ at $t = 0$, where d_i is the signed distance to the boundary (i.e., to the closest point on the boundary) then, at least initially, we have

$$\frac{\partial\phi_i}{\partial t} = \gamma_i \Delta\phi_i - e_i - \lambda\left(\sum_{i=1}^{n} H(\phi_i) - 1\right) \tag{2.17a}$$

$$\lambda = \frac{\sum_{i=1}^{n} \int\int_D \delta(\phi_i)(\gamma_i \Delta\phi_i - e_i)(\sum_{j=1}^{n} H(\phi_j) - 1)\, dx\, dy}{\sum_{i=1}^{n} \int\int_D \delta(\phi_i)(\sum_{j=1}^{n} H(\phi_j) - 1)^2\, dx\, dy}. \tag{2.17b}$$

In [16] a simple reinitialization procedure was given to replace each φ_i by d_i at the beginning of each discretization. We shall use that reinitialization here, describe it in the next section, and discuss related matters in the Appendix. This reinitialization corresponds to adding a set of constraints to the constrained minimization problem in Theorem 2.1 of the form:

$$|\nabla\varphi_i| \equiv 1, \quad i = 1, \ldots, n \tag{2.18}$$

which is an alternative way of specifying $\varphi_i = d_i$. This removes the nonuniqueness of φ in Remark 2.4 and does not change the interface motion.

Remark 2.6. The gradient-projection method minimizing $\int f(\varphi(x))\,dx$, such that $\int g(\varphi(x))\,dx = 0$, using $t =$ time as the descent variable, leads to

$$\varphi_t = -f_\varphi - \lambda g_\varphi, \tag{2.19a}$$

where

$$\lambda = -\frac{\int g_\varphi f_\varphi}{\int g_\varphi^2} \tag{2.19b}$$

with $\int g(\varphi) = 0$ at $t = 0$. Thus, Schwarz' inequality implies that $\int f(\varphi(x, t))\,dx$ is decreasing as long as $g_\varphi \neq 0$, since

$$\frac{d}{dt}\int f(\varphi) = -\int f_\varphi^2 + \frac{(\int f_\varphi g_\varphi)^2}{\int g_\varphi^2}.$$

Thus, the constraint term must not be degenerate, i.e., $g_\varphi \not\equiv 0$ if $\int g(\varphi) = 0$. This is one of the many equivalent reasons why satisfying the constraint (2.5) is too much to hope for; yet (2.6) can be obtained.

Remark 2.7. In our calculations we have replaced the boundary condition (2.17b) by nonreflecting boundary conditions approximating $(\Delta x)^2(\partial^2\varphi/\partial n^2) = 0$ at the boundary. This minimizes the effects of the boundary.

Remark 2.8. We have begun experimenting with the original descent method, i.e., where $\delta(\varphi_i)$ is used rather than $|\nabla\varphi_i|$ in (2.12a), (2.12b) and in the analogue of (2.14). Surprisingly, preliminary results are excellent. We shall discuss this in future work.

The framework we have set up here is quite general. We can easily add more constraints and change the energy functional. For example, in a domain decomposition framework, we may be given a density function $\rho(x, y) > 0$ for the density of node points in each subdomain and $\gamma(x, y) > 0$ for the communication cost per unit length of a decomposition cut. The optimal domain decomposition will have a required number of nodes in each subdomain and will have the minimum communication cost across interfaces. In two dimensions the problem can be formulated as (see [18])

Minimize

$$E = \sum_{i=1}^{n}\int\int \delta(\phi_i(x, y))|\nabla\phi_i(x, y)|\gamma(x, y)\,dx\,dy, \tag{2.20a}$$

Subject to

$$\frac{1}{2}\int\int\left(\sum_{i=1}^{n} H(\phi_i(x, y)) - 1\right)^2 dx\,dy = \varepsilon \tag{2.20b}$$

$$\int\int H(\phi_i(x, y))\rho(x, y)\,dx\,dy = A_i \quad (i = 1, ..., n-1). \tag{2.20c}$$

Using the gradient projection method (after rescaling) leads us to

$$\frac{\partial\phi_i}{\partial t} = |\nabla\phi_i|\left(\gamma\kappa_i + \frac{\nabla\gamma\cdot\nabla\phi_i}{|\nabla\phi_i|} - \mu_i\rho - \lambda\left(\sum_{j=1}^{n} H(\phi_j) - 1\right)\right), \tag{2.21a}$$

with $\mu_n = 0$, where the Lagrange multipliers λ, μ_i satisfy a linear system,

$$(m_{ij})_{(n)\times(n)}\begin{pmatrix}\lambda\\ \vdots\\ \mu_{n-1}\end{pmatrix} = \begin{pmatrix}b_1\\ \vdots\\ b_n\end{pmatrix}, \tag{2.21b}$$

where

$$\begin{aligned}
m_{11} &= \textstyle\sum_{i=1}^{n}\int\int \delta(\phi_i)|\nabla\phi_i|(\sum_{j=1}^{n} H(\phi_j) - 1)^2\,dx\,dy\\
m_{ii} &= \int\int \delta(\phi_i)|\nabla\phi_{i-1}|\rho^2\,dx\,dy, && i = 2, ..., n\\
m_{i1} &= m_{1i} = \int\int \delta(\phi_{i-1})|\nabla\phi_{i-1}|\\
&\quad \rho(\textstyle\sum_{j=1}^{n} H(\phi_j) - 1)\,dx\,dy, && i = 2, ..., n\\
m_{ij} &= 0, && \text{otherwise.}
\end{aligned}$$

The matrix (m_{ij}) is symmetric positive definite because the constraints are independent (a general consequence of the gradient-projection method), and

$$\begin{aligned}
b_1 &= \sum_{i=1}^{n}\int\int \delta(\phi_i)|\nabla\phi_i|\\
&\quad \left(\gamma\kappa_i + \frac{\nabla\gamma\cdot\nabla\phi_i}{|\nabla\phi_i|}\right)\left(\sum_{j=1}^{n} H(\phi_j) - 1\right)dx\,dy\\
b_i &= \int\int \delta(\phi_{i-1})|\nabla\phi_{i-1}|\rho\\
&\quad \left(\gamma\kappa_{i-1} + \frac{\nabla\gamma\cdot\nabla\phi_{i-1}}{|\nabla\phi_{i-1}|}\right)dx\,dy, \quad i = 2, ..., n,
\end{aligned} \tag{2.21c}$$

where

$$\kappa_i = -\nabla \cdot \left(\frac{\nabla \phi_i}{|\nabla \phi_i|} \right) = \text{local curvature of the interface.} \tag{2.21d}$$

3. NUMERICAL IMPLEMENTATION FOR MULTIPHASE MOTION

The numerical implementation of (2.12), (2.13) is simple, but requires much of the modern level set technology. The algorithm can be summarized in four steps:

Step 1. Update the Lagrange multiplier λ by (2.14)

$$\lambda^{(m+1)} = \frac{\sum_{i=1}^{n} \int\int_D \delta(\phi_i^{(m)}) |\nabla \phi_i^{(m)}| \left(\gamma_i \nabla \cdot \left(\frac{\nabla \phi_i^{(m)}}{|\nabla \phi_i^{(m)}|} \right) - e_i \right) \left(\sum_{j=1}^{n} H(\phi_j^{(m)}) - 1 \right) dx\, dy}{\sum_{i=1}^{n} \int\int_D \delta(\phi_i^{(m)}) |\nabla \phi_i^{(m)}| \left(\sum_{j=1}^{n} H(\phi_j^{(m)}) - 1 \right)^2 dx\, dy}. \tag{3.1}$$

Step 2. Advance ϕ_i by the evolution PDE (2.12). A simple time stepping algorithm is

$$\frac{\phi_i^{(m+1)} - \phi_i^{(m)}}{\Delta t} + |\nabla \phi_i^{(m)}| \left(e_i + \lambda^{(m+1)} \left(\sum_{j=1}^{n} H(\phi_j^{(m)}) - 1 \right) \right) = \gamma_i |\nabla \phi_i^{(m)}| \nabla \cdot \left(\frac{\nabla \phi_i^{(m)}}{|\nabla \phi_i^{(m)}|} \right). \tag{3.2}$$

We generally use more accurate and robust Runge–Kutta-type time discretizations; see, e.g., (3.9). Also, recall that in (3.1) and (3.2), if any $\gamma_i = 0$ we replace it by $\gamma_i = \Delta x C$, with $C = O(1)$.

Step 3. Let $d_i^0 = \phi_i^{(m+1)}$; reinitialize $\phi_i^{(m+1)}$ to be the signed distance function, using several iterations of the following discretized PDE (see [16]):

$$\frac{d_i^{(m+1)} - d_i^{(m)}}{\Delta t} + \text{sign}(d_i^{(0)})(|\nabla d_i^{(m)}| - 1) = 0. \tag{3.3}$$

Step 4. Check whether the solution is stationary,

$$Q \equiv \frac{\sum_{i=1}^{n} \sum_{|(\phi_i)_{jk}^{(m)}| < B} |(\phi_i)_{jk}^{(m+1)} - (\phi_i)_{jk}^{(m)}|}{\sum_{i=1}^{n} M_i},$$

where $M_i \equiv$ number of grid points where $|(\phi_i)_{jk}^{(m)}| < B$, $B = c\,\Delta x$ (we have taken the constant $c = 1$ in our experiments). If $Q \le (\Delta t)(\Delta x)^2$ then it is stationary and we stop, else we go back to step 1.

This procedure involves a highly nonlinear partial differential equation restricted to a manifold. There are some nontrivial numerical details which we now address.

Step 1. We approximate the Heaviside and delta functions by C^2 (respectively C^1) functions as in [11, 16, 2]:

$$H_\alpha(x) = \begin{cases} 1, & x > \alpha \\ 0, & x < -\alpha \\ \frac{1}{2}\left[1 + \frac{x}{\alpha} + \frac{1}{\pi} \sin\left(\frac{\pi x}{\alpha} \right) \right], & |x| \le \alpha; \end{cases} \tag{3.4a}$$

$$\delta_\alpha(x) = \frac{d}{dx} H_\alpha(x) = \begin{cases} 0, & |x| > \alpha \\ \frac{1}{2\alpha}\left[1 + \cos\left(\frac{\pi x}{\alpha} \right) \right], & |x| \le \alpha. \end{cases} \tag{3.4b}$$

In our calculations we took $\alpha = \Delta x$.

In (3.1), $\int\int \delta(\varphi) |\nabla \varphi| \nabla \cdot (\nabla \varphi / |\nabla \varphi|)$ is the average of mean curvature at the front. Since the width of the support of our approximate delta function is positive, we would get some average of curvature of level sets near the front if we were to literally use this formula. We get better results by using

$$\kappa = \frac{\Delta \varphi}{1 - \varphi\, \Delta \varphi}. \tag{3.5}$$

This appears, e.g., in [4]; we discuss it in the Appendix. This (nonobvious) formula, when φ is the distance function, is constant normal to the front and, of course, gives the correct value at the front.

Standard central difference formulae are used for all of the remaining terms in (3.1).

Step 2. We view (3.2) as an approximation to a Hamilton–Jacobi equation with curvature regularization of the form

$$\varphi_t + |\nabla \varphi| (a(x, y, t)) = \gamma |\nabla \varphi| \nabla \cdot \left(\frac{\nabla \varphi}{|\nabla \varphi|} \right) \tag{3.6}$$

for $\gamma \ge 0$. High order ENO (essentially nonoscillatory) approximations to equations of this type have been obtained in [9, 10] and are needed to avoid oscillations for γ small. We use the following:

(i) if $e_i + \lambda(\sum_{j=1}^{n} H(\phi_j) - 1) \geq 0$ then

$$|\nabla \phi_{jk}| = \sqrt{((\max(D_-^x \phi_{jk}, 0))^2 + (\min(D_+^x \phi_{jk}, 0))^2) + (\max(D_-^y \phi_{jk},))^2 + (\min(D_+^y \phi_{jk}, 0))^2)} \tag{3.7}$$

(ii) if $e_{\mathrm{i}} + \lambda(\sum_{j=1}^{n} H(\phi_j) - 1) < 0$ then

$$|\nabla \phi_{jk}| = \sqrt{((\min(D_-^x \phi_{jk}, 0))^2 + (\max(D_+^x \phi_{jk}, 0))^2) + (\min(D_-^y \phi_{jk}, 0))^2 + (\max(D_+^y \phi_{jk}, 0))^2)},$$

where j, k are the index for the x and y coordinates and

$$D_-^x \phi_{jk} = \frac{\phi_{j,k} - \phi_{j-1,k}}{\Delta x} + \frac{\Delta x}{2} m \left[\frac{\phi_{j+1,k} - 2\phi_{j,k} + \phi_{j-1,k}}{(\Delta x)^2}, \frac{\phi_{j,k} - 2\phi_{j-1,k} + \phi_{j-2,k}}{(\Delta x)^2} \right]$$

$$D_+^x \phi_{jk} = \frac{\phi_{j+1,k} - \phi_{j,k}}{\Delta x} - \frac{\Delta x}{2} m \left[\frac{\phi_{j+2,k} - 2\phi_{j+1,k} + \phi_{j,k}}{(\Delta x)^2}, \frac{\phi_{j+1,k} - 2\phi_{j,k} + \phi_{j-1,k}}{(\Delta x)^2} \right]$$

$$D_-^y \phi_{jk} = \frac{\phi_{j,k} - \phi_{j,k-1}}{\Delta y} + \frac{\Delta y}{2} m \left[\frac{\phi_{j,k+1} - 2\phi_{j,k} + \phi_{j,k-1}}{(\Delta y)^2}, \frac{\phi_{j,k} - 2\phi_{j,k-1} + \phi_{j,k-2}}{(\Delta y)^2} \right]$$

$$D_+^y \phi_{jk} = \frac{\phi_{j,k+1} - \phi_{j,k}}{\Delta y} - \frac{\Delta y}{2} m \left[\frac{\phi_{j,k+2} - 2\phi_{j,k+1} + \phi_{j,k}}{(\Delta y)^2}, \frac{\phi_{j,k+1} - 2\phi_{j,k} + \phi_{j,k-1}}{(\Delta y)^2} \right]$$

$$m[x, y] = \begin{cases} x & \text{if } |x| \leq |y|, x \cdot y > 0 \\ y & \text{if } |x| > |y|, x \cdot y > 0. \\ 0 & \text{if } x \cdot y \leq 0. \end{cases}$$

The curvature term is approximated by using

$$\nabla \cdot \left(\frac{\nabla \phi}{|\nabla \phi|} \right) = \left(\frac{\phi_x}{|\nabla \phi|} \right)_x + \left(\frac{\phi_y}{|\nabla \phi|} \right)_y \tag{3.8}$$

so

$$\nabla \cdot \left(\frac{\nabla \phi}{|\nabla \phi|} \right)_{jk} = \left[\left(\frac{\phi_x}{|\nabla \phi|} \right)_{j+1/2,k} - \left(\frac{\phi_x}{|\nabla \phi|} \right)_{j-1/2,k} \right] \Big/ \Delta x + \left[\left(\frac{\phi_y}{|\nabla \phi|} \right)_{j,k+1/2} - \left(\frac{\phi_y}{|\nabla \phi|} \right)_{j,k-1/2} \right] \Big/ \Delta y,$$

where

$$\left(\frac{\phi_x}{|\nabla \phi|} \right)_{j+1/2,k} = \frac{(\phi_{j+1,k} - \phi_{j,k})/\Delta x}{\sqrt{[(\phi_{j+1,k} - \phi_{j,k})/\Delta x]^2 + \{\frac{1}{2}[(\phi_{j,k+1} - \phi_{j,k-1})/2\,\Delta y + (\phi_{j+1,k+1} - \phi_{j+1,k-1})/2\,\Delta y]\}^2}}$$

$$\left(\frac{\phi_x}{|\nabla \phi|} \right)_{j-1/2,k} = \frac{(\phi_{j,k} - \phi_{j-1,k})/\Delta x}{\sqrt{[(\phi_{j,k} - \phi_{j-1,k})/\Delta x]^2 + \{\frac{1}{2}[(\phi_{j-1,k+1} - \phi_{j-1,k-1})/2\,\Delta y + (\phi_{j,k+1} - \phi_{j,k-1})/2\,\Delta y]\}^2}}$$

$$\left(\frac{\phi_y}{|\nabla \phi|} \right)_{j,k+1/2} = \frac{(\phi_{j,k+1} - \phi_{j,k})/\Delta y}{\sqrt{\{\frac{1}{2}[(\phi_{j+1,k} - \phi_{j-1,k})/2\,\Delta x + (\phi_{j+1,k+1} - \phi_{j-1,k+1})/2\,\Delta x]\}^2 + [(\phi_{j,k+1} - \phi_{j,k})/\Delta y]^2}}$$

$$\left(\frac{\phi_y}{|\nabla \phi|} \right)_{j,k-1/2} = \frac{(\phi_{j,k} - \phi_{j,k-1})/\Delta y}{\sqrt{\{\frac{1}{2}[(\phi_{j+1,k-1} - \phi_{j-1,k-1})/2\,\Delta x + (\phi_{j+1,k} - \phi_{j-1,k})/2\,\Delta x]\}^2 + [(\phi_{j,k} - \phi_{j,k-1})/\Delta y]^2}}.$$

To obtain a high order accurate scheme in time, we replace the forward Euler-like discretization of (3.2) by using a semi-discrete approximation

$$\frac{\partial}{\partial t} \phi_{jk} = -L[\phi, j, k]$$

and certain Runge–Kutta-type schemes (see Shu and Osher [15]). For example, a second-order essentially non-oscillatory Runge–Kutta algorithm is Heun's method,

$$\begin{aligned} \overline{\phi}_{jk}^{m+1} &= \phi_{jk}^m - \Delta t L[\phi^m, j, k] \\ \phi_{jk}^{m+1} &= \frac{1}{2} \phi_{jk}^m + \frac{1}{2} \overline{\phi}_{jk}^{m+1} - \frac{\Delta t}{2} L[\tilde{\phi}_i^{m+1}, j, k] \end{aligned} \tag{3.9}$$

which has a slightly reduced CFL (time step) restriction from the underlying monotone scheme.

At the boundary of our computational domain, we use the nonreflecting boundary condition $\partial^2\varphi/\partial n^2 = 0$.

Step 3. The original level set formulation [9] did not require anything special about the nature of φ, other than that it be sufficiently smooth. In a number of works [16, 2, 6], it was found to be quite desirable that φ be constantly updated to be a signed distance, at least near the front. A fast reinitialization algorithm was given in [16]; we repeat it here. In our setting, the singular distributions $\delta(\varphi)$ and $H(\varphi)$ are involved in the motion (as was true in [16, 2]) and this reinitialization step is quite important.

In (3.3) we approximate the sign function by

$$\operatorname{sign}(d_i^0) = \frac{d_i^{(0)}}{\sqrt{(d_i^{(0)})^2 + (\Delta x)^2}}.$$

This equation is of the type (3.6) with $\gamma = 0$ and $a(x, y, t) = \operatorname{sign}(d_i^0)$. Thus the numerical procedure of (3.7), (3.8) is used (with the same boundary conditions, using the appropriate $a(x, y, t)$).

The last technical detail involves the constraint near multiple junctions. Since the numerical Heaviside function has the property that $H_\alpha(0) = \frac{1}{2}$, we require that the constraint satisfy

$$\sum_{i=1}^{n} H(\varphi_i(x)) - \frac{n}{2} = 0 \tag{3.10}$$

for $|\varphi_i(x)|$ sufficiently small for each i. This is done only for the first few time iterations. Since a triple point is stable, we replace $n/2$ by $3/2$ after a few iterations, again, only in regions in which the $|\varphi_i(x)|$ are small. This affects only the values of $\lambda^{(m+1)}$.

Remark 3.1. Using this numerical implementation we find a very small vacuum region (and almost no overlap) and no growth of vacuum or overlap in time.

Remark 3.2. We replaced each γ_i by $\varepsilon\gamma_i$, and let $\varepsilon \to 0$ to see if our numerical scheme picks out the unique VST (vanishing surface tension; see [12]) solution computed with all the $\gamma_i \equiv 0$. It turns out that it does, but we do need the numerical lower bound $\gamma_i \geq C\,\Delta x$.

Remark 3.3. An implicit in time scheme would be useful to remove the $\Delta t \sim (\max \gamma_i)(\Delta x)^2$ parabolic stability restriction. However, it should be noted that the nonlinear stiff terms involving $H(\varphi_j)$ also restrict the time step. Thus we have not yet made this method implicit in time.

Remark 3.4. The angle condition for a triple point, (1.2), is obtained instantaneously (as predicted), i.e., after a very small number of iterations.

Remark 3.5. A fundamental idea, whose time has come in problems like ours, is to use the level set formulation only near the zero level sets themselves, thus cutting down the numerical work by an order of magnitude. This was discussed by Adalsteinsson and Sethian in [1], and a method was proposed and successfully implented for the single level set case. We have in [18] developed a somewhat simpler method which was used here in this multiphase case and which was applied to three-dimensional problems in [18]. Typical calculations in the next section involving three phases, 5×10^3 iterations and a 100×100 grid took $2\frac{1}{2}$ h on our SPARC 10 machine. This is a speedup of at least a factor of 5 over the straightforward, global method. More generally, this results in an $O(N)$ speedup for the time of the method applied to an $N \times N$ grid.

4. NUMERICAL RESULTS

In all our numerical experiments we use

$$D = [0, 1] \times [0, 1], \quad \Delta x = \Delta y = 10^{-2}, \quad \Delta t = 10^{-5}.$$

In the first experiment, we study the motion of the interfaces under constant velocity caused only by the difference of bulk energy ($v_{ij} = e_i - e_j$). As is shown by Reitich and Soner in [12], there is no unique solution in this case and the VST solution (letting $\gamma_i \to 0$) picks up the unique solution which satisfies their weak angle conditions at the triple point. We start with a case described in [12]: three straight lines meeting at 120° (see the right side of Figs. 3a,b,c). We set $e_1 = e_2 = 5$, $e_3 = 1$. In our first experiment displayed in Fig. 3a we use a 100×100 grid and set $\gamma_1 = \gamma_2 = \gamma_3 = 0.01$. In Fig. 3b we set $\gamma_1 = \gamma_2 = \gamma_3 = 0.005$ and a 150×150 grid. Finally, in Fig. 3c we use $\gamma_1 = \gamma_2 = \gamma_3 = 0.0025$ and a 200×200 grid. In all cases the left sides of these figures agree with the VST solution of [12].

In Fig. 3d we set $e_1 = 2.5$, $e_2 = 1$, $e_3 = 0.5$, $\gamma_1 = \gamma_2 = \gamma_3 = 0.005$ on a 200×200 grid. then each interface moves with a different velocity. The 120° relation is maintained at the triple point which means in this case that we have the VST solution.

In the second numerical experiment, we start with Fig. 4a. In Fig. 4b we set

$$\gamma_1 = \gamma_2 = 0, \quad \gamma_3 = 1, \quad e_1 = e_2 = e_3 = 0,$$

which makes $\theta_3 = 180°$ by the angle relation (2.7) at the triple point. We have zero bulk energy. Thus, we only minimize the length of the boundary of the third domain. At $t = 0.05$, we get Fig. 4(b). Since the starting figure already has $\theta_3 = 180°$ (the boundary of the third domain is a straight line), we would expect no motion at all at the triple point. This agrees with our result. This also shows that our numerical scheme has little artificial dissipation.

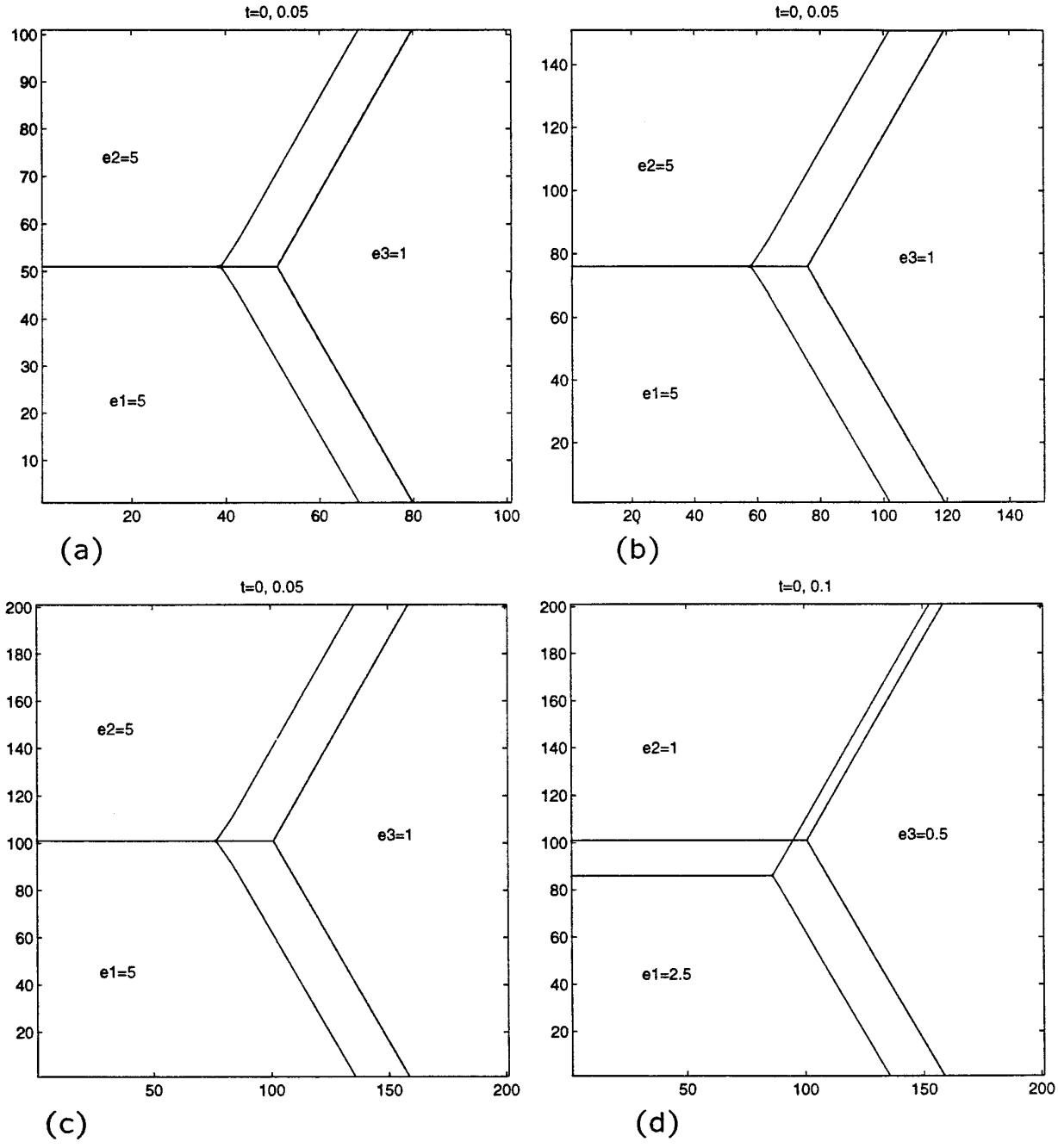

FIG. 3. (a) $\gamma_1 = \gamma_2 = \gamma_3 = 0.01$; (b) $\gamma_1 = \gamma_2 = \gamma_3 = 0.005$; (c) $\gamma_1 = \gamma_2 = \gamma_3 = 0.0025$; (d) $\gamma_1 = \gamma_2 = \gamma_3 = 0.005$.

In Fig. 4c we set

$$\gamma_1 = (\sqrt{3}-1)/4, \quad \gamma_2 = (\sqrt{3}+1)/4, \quad \gamma_3 = (3-\sqrt{3})/4,$$
$$e_1 = e_2 = e_3 = 0.$$

We would expect $\theta_1 = \pi/2$, $\theta_2 = 5\pi/6$, $\theta_3 = 2\pi/3$ at the triple point and no convection due to the bulk energy. This is shown in Fig. 4c, at $t = 0.05$.

In the most general case, we have both different bulk energies and also surface tension between each phase. In Fig. 4d, we use

$$\gamma_1 = (\sqrt{3}-1)/4, \quad \gamma_2 = (\sqrt{3}+1)/4, \quad \gamma_3 = (3-\sqrt{3})/4,$$
$$e_1 = 10, \quad e_2 = 5, \quad e_3 = 1.$$

So we not only have the same angle condition as in case

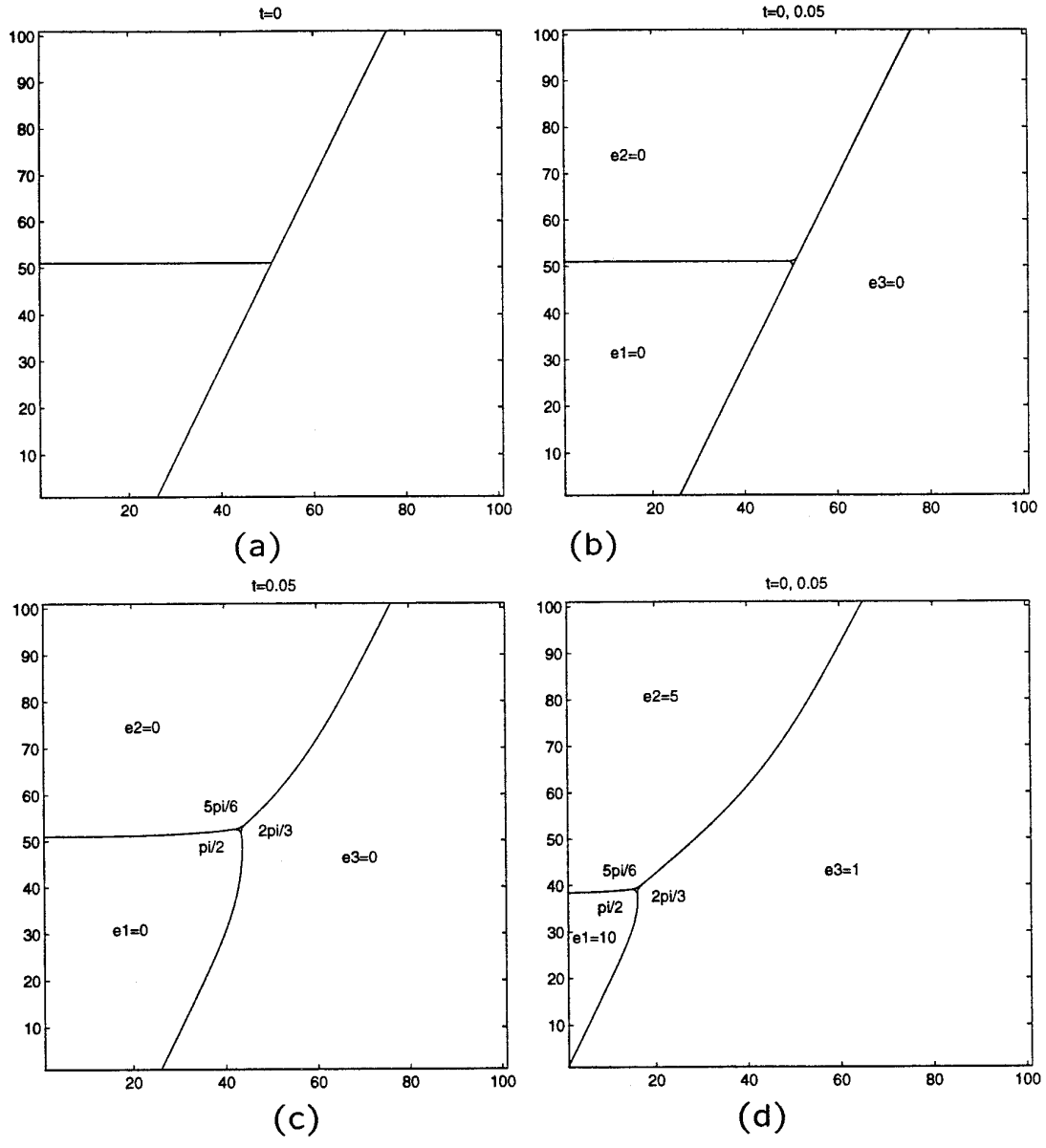

FIG. 4. (a), (b) $\gamma_1 = \gamma_2 = 0$, $\gamma_3 = 1$; (c), (d) $\gamma_1 = (\sqrt{3} - 1)/4$, $\gamma_2 = (\sqrt{3} + 1)/4$, $\gamma_3 = (3 - \sqrt{3})/4$.

(b), but we also see the convection of the triple point by the difference in bulk energy ($e_1 > e_2 > e_3$). The area of the first domain is shrinking and the area of the second domain is growing.

In the third experiment, we deal with the case where two interfaces merge and topological change occurs. We start with two interfaces with sharp corners, Fig. 5a at $t = 0$. We set $e_1 = 1$, $e_2 = 10$, $e_3 = 5$, and $\gamma_1 = \gamma_2 = \gamma_3 = 0$. At $t = 0.02$ we get Fig. 5b and at $t = 0.05$ we get Fig. 5(c). We see that this level set approach treats topological changes very easily.

In Fig. 5d we set $\gamma_1 = \gamma_2 = \gamma_3 = 0.01$. With small viscosity, we get almost the same result as without viscosity at all, in this case. Thus, we again recommend using $O(\Delta x)$ viscosity in these calculations to be safe.

In the next experiment, we see how a multiple junction evolves into several triple points. We start with Fig. 6a, with all $\gamma_i = 1$, $e_i = 0$. As time goes on, we get Fig. 6b and Fig. 6c and Fig. 6d.

Figure 7 shows the effect of the curvature term in the evolution procedure. We see, for $e_1 = 3$, $e_2 = 5$, and $e_3 = 1$ the results with differing γ's, the same γ for each interface. Figure 7a shows the result with $\gamma = 1$ for a 100×100 grid. The curvature straightens out the initial bump in Γ_{23} and yields approximately 120° angles. Figure 7b shows the results for $\gamma = 0.1$ on the same grid. The bump is less straight

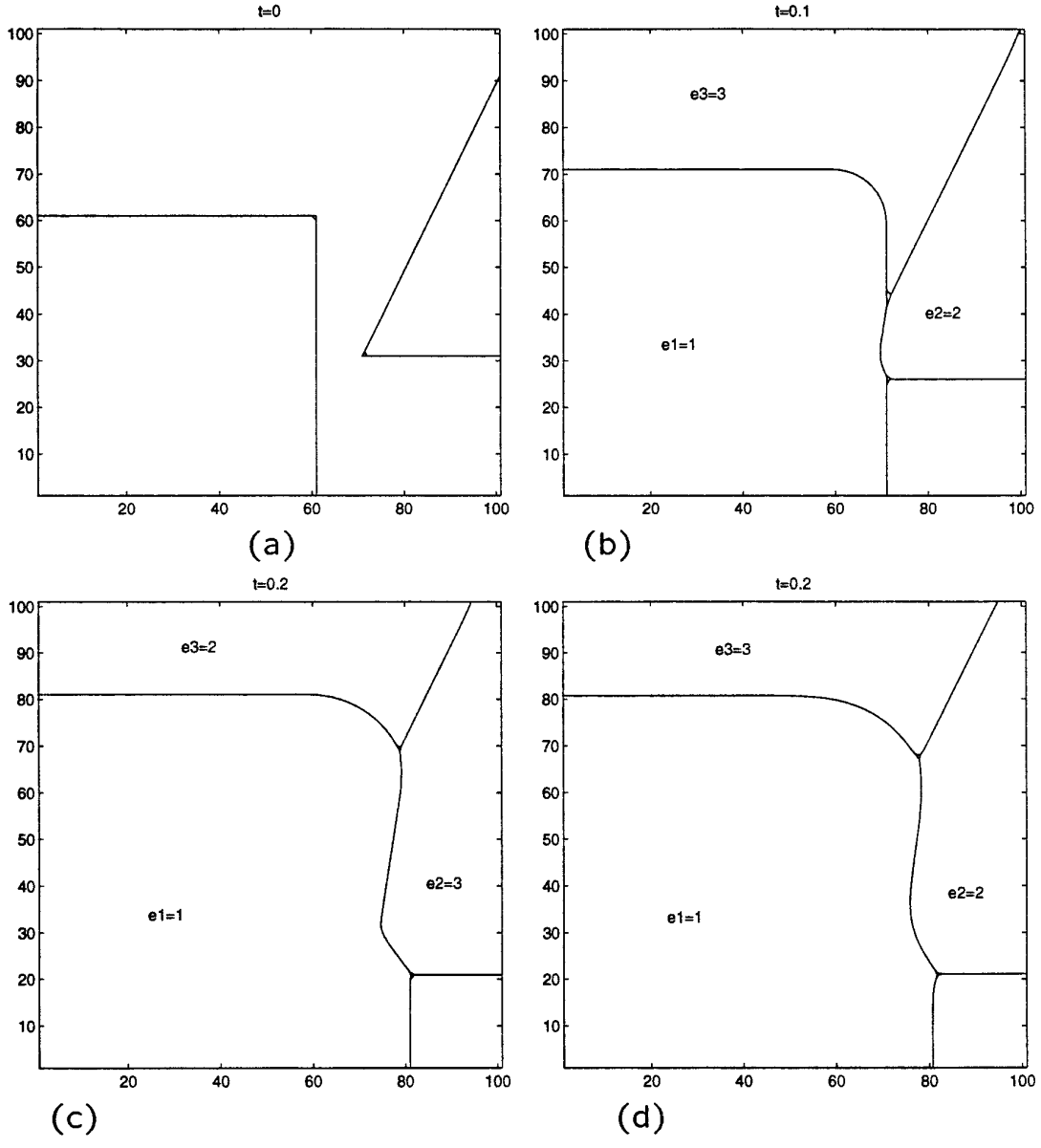

FIG. 5. (a)–(c) $\gamma_1 = \gamma_2 = \gamma_3 = 0$; (d) $\gamma_1 = \gamma_2 = \gamma_3 = 0.01$.

and the 120° angle is valid only in a "boundary layer" near the triple point. Figure 7c shows the results for $\gamma = \Delta x = 0.01$. The bump is still visible, and this is clearly regularized motion by a constant. Finally, Fig. 7d has $\gamma = \Delta x/5$, with $\Delta x = 0.005$. We are stretching the limits of our slight regularization and we see that typical development of a "kink" in the inviscid motion case.

APPENDIX: SOME NEW LEVEL SET METHODOLOGY

To make each $\phi(x, t)$ unique and well behaved numerically, we require that it be the signed distance from the front, i.e., that $|\nabla\phi(x, t)| = 1$. This does not remain true in general and is very important, especially when $\mathbf{v}(x, t)$ involves singularities at the front. Here, we shall give some ideas on how to maintain φ as a distance function. (In this section the results apply in an arbitrary number l, of space dimensions. We simply denote a point in R^l by x).

LEMMA A1. *Let $v_n = \mathbf{v} \cdot \nabla\varphi$ be the normal velocity of each level set, and set $\varphi(x, 0)$ to be the signed distance function. Then φ remains as a signed distance function iff $\nabla v_n \cdot \nabla\varphi \equiv 0$.*

Proof.

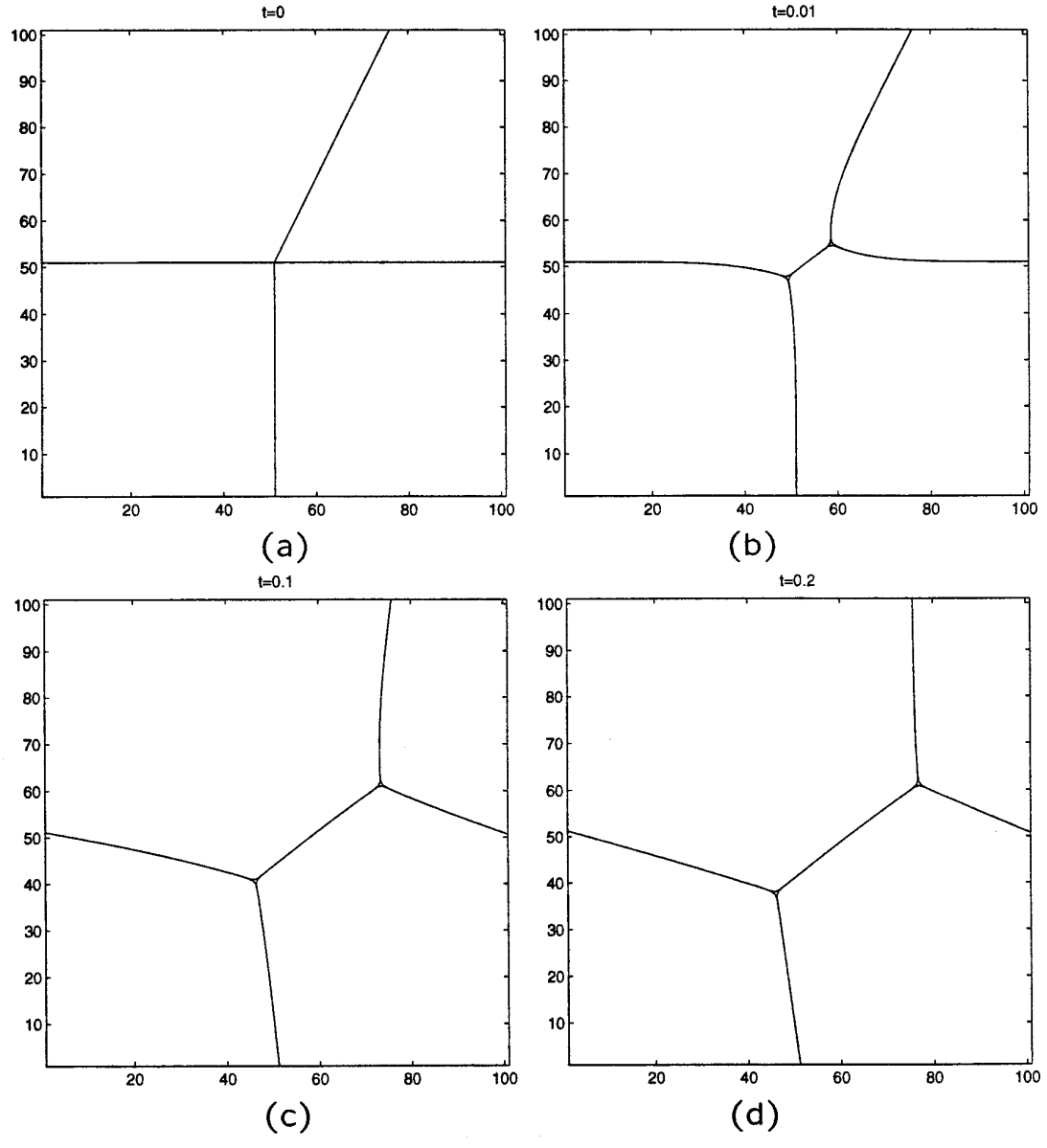

FIG. 6. $\gamma_i = 1$; $e_i = 0$.

$$\frac{\partial}{\partial t}|\nabla\varphi|^2 = 2\,\nabla\varphi\cdot\nabla\varphi_t = -2(\nabla\varphi\cdot\nabla v_n)|\nabla\varphi| \\ -2v_n(\nabla\varphi\cdot\nabla|\nabla\varphi|). \tag{A.1}$$

Thus, $|\nabla\varphi| \equiv 1$ for later time iff the "source term" vanishes; i.e., $\nabla\varphi\cdot\nabla v_n \equiv 0$.

We show that the previous method of reinitialization [16], as described in Section 3, is equivalent to modifying $v_n(x, t)$ off the front. The reinitialization procedure comes from

(i) Evolve $\varphi(x, t)$, starting from a distance function, φ^{old}, via

$$\varphi_t + \mathbf{v}\cdot\nabla\varphi = 0, \tag{A.1a}$$

i.e.,

$$\varphi^{\text{new}} = \varphi^{\text{old}} - v_n\,\Delta t + O(\Delta t)^2. \tag{A.1b}$$

(ii) Do the reinitialization on φ^{new} as usual

$$\varphi^{(m+1)} = \varphi^{(m)} + \text{sign}(\varphi^{(0)}(1 - |\nabla\varphi^{(m)}|)\,\Delta\tau + O(\Delta\tau)^2 \tag{A.2a}$$

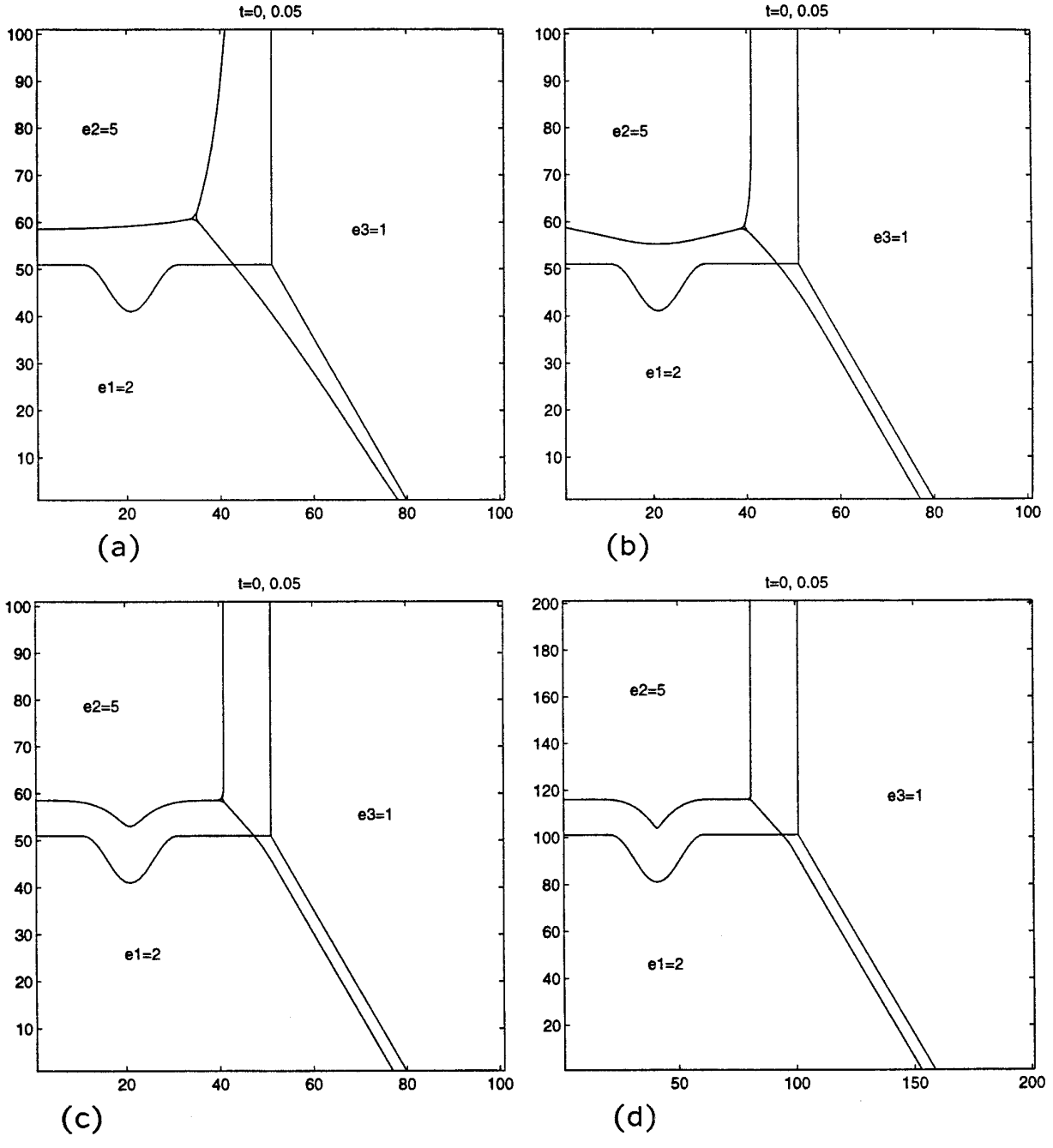

FIG. 7. (a) $\gamma_1 = \gamma_2 = \gamma_3 = 1$; (b) $\gamma_1 = \gamma_2 = \gamma_3 = 0.1$; (c) $\gamma_1 = \gamma_2 = \gamma_3 = 0.01$; (d) $\gamma_1 = \gamma_2 = \gamma_3 = 0.001$.

with

$$\varphi^{(0)} = \varphi^{\text{new}}. \tag{A.2b}$$

We have

LEMMA A2. *The reinitialization step* (A2) *is equivalent to extending* $v_n(x, t)$ *off the front so that*

$$\nabla\varphi \cdot \nabla v_n = 0$$

on the front.

Proof. From (A.2)

$$\nabla\phi^{(0)} = \nabla\phi^{\text{new}} = \nabla\phi^{\text{old}} - \nabla v_n \,\Delta t + o((\Delta t)^2).$$

We next use Taylor expansion and the fact that

$$
\begin{aligned}
|\nabla\phi^{\text{old}}| = 1 = \\
\phi^{(1)} &= \phi^{(0)} + \text{sign}(\phi^{(0)})(1 - |\nabla\phi^{(0)}|)\,\Delta\tau + o(\Delta t^2) \\
&= \phi^{\text{old}} - v_n\,\Delta t + \text{sign}(\phi^{(0)}) \\
&\quad (1 - \sqrt{(\nabla\phi^{\text{old}} - \nabla v_n\,\Delta t)\cdot(\nabla\phi^{\text{old}} - \nabla v_n\,\Delta t)})\,\Delta\tau + o(\Delta t)^2 \\
&= \phi^{\text{old}} - v_n\,\Delta t + \text{sign}(\phi^{(0)}) \\
&\quad \left[1 - \left(|\nabla\phi^{\text{old}}| - \frac{\nabla\phi^{\text{old}}\cdot\nabla v_n}{|\nabla\phi^{\text{old}}|}\Delta t + O(\Delta t)^2\right)\right]\Delta\tau + o(\Delta t)^2 \\
&= \phi^{\text{old}} - \left[v_n - \text{sign}(\varphi^{\text{old}})\frac{\nabla\phi^{\text{old}}\cdot\nabla v_n}{|\nabla\phi^{\text{old}}|}\Delta\tau\right]\Delta t + O((\Delta t)^2)
\end{aligned}
$$

by induction,

$$\phi^{(m)} = \phi^{\text{old}} - v_n^{(m)}\,\Delta\tau + o(\Delta t)^2,$$

where

$$v_n^{(m)} = v_n^{(m-1)} - \text{sign}(\phi^{\text{old}})\frac{\nabla\phi^{\text{old}}\cdot\nabla v_n^{(m-1)}}{|\nabla\phi^{\text{old}}|}\Delta\tau$$

which means, as $m \to \infty$, $v_n^{(m)}(x, t)$ goes to the steady-state solution (τ independent) of

$$\frac{\partial v_n(x,t,\tau)}{\partial\tau} + \text{sign}(\phi(x,t))\frac{\nabla\phi(x,t)\cdot\nabla v_n(x,t,\tau)}{|\nabla\phi(x,t)|} = 0. \quad \blacksquare$$

We have not yet tried to implement this procedure.

Another appealing idea involves tracing the velocity back to the front—see, e.g., [4]. This is the content of the following.

LEMMA A3. *If $\varphi(x, 0)$ is the signed distance, then $\varphi(x, t)$ remain a signed distance if we use the following procedure*:

Set

$$v_n(x,t) = v_n(x - \varphi\,\nabla\varphi) = (v\cdot\nabla\varphi)(p(x)) \quad \text{(A.3a)}$$

and solve

$$\varphi_t + v_n(x - \varphi\,\nabla\varphi) = 0, \quad \text{(A.3b)}$$

where the point on the curve closest to x is

$$p(x) = x - \varphi\,\nabla\varphi. \quad \text{(A.3c)}$$

Proof.

$$
\begin{aligned}
\frac{d}{dt}|\nabla\phi|^2 &= 2\,\nabla\phi\cdot\nabla\phi_t \\
&= -2\,\nabla\phi\cdot\nabla v_n(x - \phi\,\nabla\phi, t) \\
&= -2\,\nabla\phi[I - \nabla(\phi\,\nabla\phi)]\,\nabla v_n \\
&= -[2(1 - |\nabla\phi|^2)\,\nabla\phi - \phi(\nabla|\nabla\phi|^2)]\,\nabla v_n.
\end{aligned}
$$

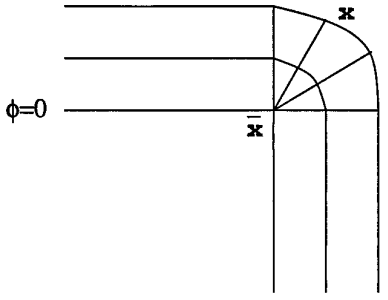

FIG. 8. Corner at the front.

Thus, if $|\nabla\varphi| \equiv 1$ initially, it remains so for a later time. ∎

The PDE (A.3b) is highly nonlinear and difficult to analyze. The numerical implementation is difficult to carry out in the presence of corners, since the corner can be the preimage of a whole section of a curve under the map $x \to x - \varphi\,\nabla\varphi$. See Fig. 8.

The formula (A.3a) simplies and becomes useful if v_n is a function of curvature; see e.g., [4].

LEMMA A4. *If $\phi(x, t)$ is a signed distance and smooth, then*

$$\kappa(x - \phi\,\nabla\phi) = \frac{-\Delta\phi(x)}{1 - \phi(x)\,\Delta\phi(x)}. \quad \text{(A.4)}$$

Proof. Let $\bar{x} = x - \phi(x)\,\nabla\phi(x)$ (see Fig. 9),

$$\kappa(x) = \frac{1}{r(\bar{x}) - \phi(x)} = -\nabla\cdot\left(\frac{\nabla\phi(x)}{|\nabla\phi(x)|}\right) = -\nabla\phi(x)$$

$$r(\bar{x}) = \phi(x) - \frac{1}{\Delta\phi(x)},$$

so

$$\kappa(\bar{x}) = \frac{1}{r(\bar{x})} = \frac{-\Delta\phi(x)}{1 - \phi(x)\,\Delta\phi(x)}.$$

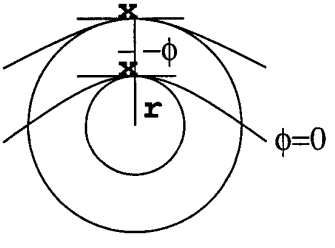

FIG. 9. Curvature using distance function.

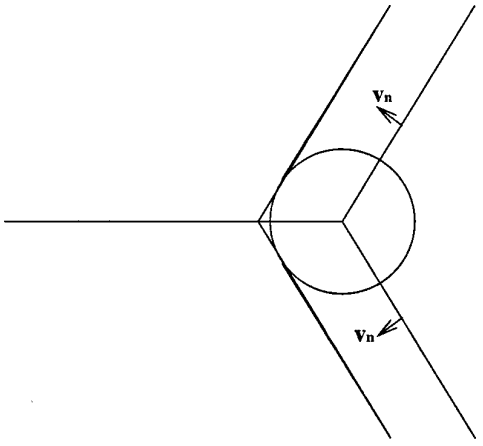

FIG. 10. Motion with constant velocity at triple point.

Remark A.1. The resulting evolution equations of the type

$$\frac{\partial \varphi}{\partial t} = F\left(\frac{\nabla \varphi}{1 - \varphi \nabla \varphi}\right) \tag{A5}$$

for $F'(x) \geq 0$ are well posed in the sense of viscosity solutions (see, e.g., [3]) if the right-hand side of (A5) is a smooth nondecreasing function of $\Delta\varphi$. This is true away from $\varphi\, \Delta\varphi = 1$.

In the special case when F is linear and increasing we have used the following implicit method to integrate (A5) (with $\Delta\varphi$ approximated by standard central differencing)

$$\frac{\varphi^{(m+1)} - \varphi^{(m)}}{\Delta t} = F\left(\frac{\Delta \varphi^{(m+1)}}{1 - \varphi^{(m)}\, \Delta \varphi^{(m)}}\right). \tag{A6}$$

When we approach the zeros of the denominator (away from the front) the scheme breaks down. Thus we replace the denominator by

$$1 - \varphi\, \Delta\varphi = \min(\varepsilon, 1 - \varphi\, \Delta\varphi) \quad \text{for small } \varepsilon > 0. \tag{A7}$$

This leaves the motion of the front unaffected.

Remark A2. The level set method corresponding to two-phase flow as devised in [9] and in many succeeding papers treats vanishing surface tension numerically by computing the viscosity solution of the inviscid problem with no explicit numerical viscosity used or needed. In this work, in order to obtain the "inviscid limit" [12] as $\gamma_i \to 0$ we need to explicitly add $O(\Delta x)$ times the length in the variational formulation (2.3b). We now show via a simple example that this is necessary; otherwise we would compute the inviscid case as in [17].

Consider the situation in Fig. 10. The initial set up is displayed on the right of that figure. The normal velocity of the curve Γ_{12} is 0 while Γ_{23} and Γ_{13} have normal velocity v_n, say, equal to one. Thus the Huygen's principle approach devised in [17] amounts to moving the boundary of Ω_3 normal to itself with unit normal velocity. This means that after time t the boundary of Ω_3 consists of all points at a distance t from the original boundary, while Γ_{12} does not move. The result can be achieved by obtaining the viscosity solution of a single level set function φ_3, solving

$$\varphi_3 + |\nabla \varphi_3| = 0 \tag{A8}$$

and the numerical methods of [9, 10] will yield the solution in [17]—see Fig. (10). Thus even though we compute φ_3 as the (viscosity) limit as $\varepsilon \downarrow 0$ of

$$\varphi_t + |\nabla \varphi| = \varepsilon |\nabla \varphi| \nabla \cdot \left(\frac{\nabla \varphi}{|\nabla \varphi|}\right),$$

the limit solution is the one in [17], not the regularized limit of Reitich and Soner in [12].

If we turn to our formulation (2.12) and let all the $\gamma_i = 0$, $i = 1, 2, 3$, we arrive at the system

$$\frac{\partial \varphi_1}{\partial t} = |\nabla \varphi_1| \left(-\lambda \left(\sum_{j=1}^{3} H(\varphi_j) - 1\right)\right) \tag{A.10a}$$

$$\frac{\partial \varphi_2}{\partial t} = |\nabla \varphi_2| \left(-\lambda \left(\sum_{j=1}^{3} H(\varphi_j) - 1\right)\right) \tag{A.10b}$$

$$\frac{\partial \varphi_3}{\partial_t} = |\nabla \varphi_3| \left(-1 - \lambda \left(\sum_{j=1}^{3} H(\varphi_j) - 1\right)\right) \tag{A.10c}$$

and in the no overlap, no vacuum case, the system is equivalent to (A.8) which again gives the result in [17], not [12]. The addition of a Δx penalty for length reverses this.

ACKNOWLEDGMENTS

The authors thank the referees for some important and constructive comments on a first draft and Fernando Reitich for carefully describing the VST limit of three phase motion to us.

REFERENCES

1. D. Adalsteinsson and J. A. Sethian, CPAM, U.C. Berkeley Report LBL 34893, PAM-598, 1993 (unpublished).
2. Y.-C. Chang, T.-Y. Hou, B. Merriman, and S. Osher, UCLA CAM Report 94-4, 1994; *J. Comput. Phys.* **124,** 449 (1996).
3. M. G. Crandall, H. Ishii, and P.-L. Lions, *Am. Math. Soc. Bull.* **27,** 1 (1992).
4. L. C. Evans and J. Spruck, *Trans. Am. Math. Soc.* **330,** 321 (1990).
5. P. Mascarenhas, UCLA CAM Report 92-33, 1992 (unpublished).
6. B. Merriman, J. Bence, and S. Osher, *J. Comput. Phys.* **112,** 334 (1994).

7. B. Merriman, J. Bence, and S. Osher, "Diffusion Generated Motion by Mean Curvature," in *AMS Selected Lectures in Math., The Comput. Crystal Grower's Workshop,* edited by J. Taylor (Am. Math. Soc., Providence, RI, 1993), p. 73.
8. S. Osher, *Proc. Int. Congress Mathematicians, Zürich, 1994,* pp. 1449–1459.
9. S. Osher and J. A. Sethian, *J. Comput. Phys.* **79,** 12 (1988).
10. S. Osher and C.-W. Shu, *SINUM* **28,** 907 (1991).
11. C. Peskin, *J. Comput. Phys.* **25,** 220 (1977).
12. F. Reitich and H. M. Soner, *Proc. Royal Soc. Edinburgh,* to appear.
13. J. G. Rosen, *J. SIAM* **9,** 514 (1961).
14. J. A. Sethian, *Commun. Math. Phys.* **101,** 487 (1985).
15. C.-W. Shu and S. Osher, *J. Comput. Phys.* **83,** 32 (1989).
16 M. Sussman, P. Smereka, and S. Osher, *J. Comput. Phys.* **114,** 146 (1994).
17. J. E. Taylor, *J. Differential Equations,* **119,** 109 (1995).
18. H.-K. Zhao, J.-P. Shao, S. Osher, T. Chan, and B. Merriman, preprint.